International Journal of Applied Pharmaceutics

ISSN- 0975-7058 Vol 16, Issue 2, 2024

Original Article

FORMULATION, CHARACTERIZATION AND OPTIMIZATION OF FOLIC ACID-TAILORED DAIDZEIN SOLID LIPID NANOPARTICLES FOR THE IMPROVED CYTOTOXICITY AGAINST COLON CANCER CELLS

SYED SUHAIB AHMED[1], MOHD ABDUL BAQI[2], MOHD ZUBAIR BABA[3], NATARAJAN JAWAHAR[1*]

[1*]Department of Pharmaceutics, JSS College of Pharmacy, JSS Academy of Higher Education and Research, Ooty, Nilgiris, Tamil Nadu, India. [2]Department of Pharmaceutical Biotechnology, JSS College of Pharmacy, JSS Academy of Higher Education and Research, Ooty, Nilgiris, Tamil Nadu, India. [3]Department of Pharmaceutical Chemistry, JSS College of Pharmacy, JSS Academy of Higher Education and Research, Ooty, Nilgiris, Tamil Nadu, India

*Corresponding author: Natarajan Jawahar; *Email: jawahar.n@jssuni.edu.in

Received: 17 Nov 2023, Revised and Accepted: 30 Dec 2023

ABSTRACT

Objective: The study aims to formulate and optimize daidzein-conjugated folic acid solid lipid nanoparticles (DZN-FA SLNs) to improve bioavailability and target site specificity for the treatment of colon cancer, a significant global health concern associated with high morbidity and mortality.

Methods: DZN-FA SLNs were prepared using the microemulsion method. They were prepared and optimized using design expert software. Physicochemical characterization like differential light scattering (DLS), Fourier transformed infrared spectroscopy (FTIR), scanning electron microscope (SEM), *In vitro* drug release and *In vitro* cell line studies and accelerated stability studies were carried out in the optimized batch formulation.

Results: The results indicated that particle size for optimized DZN-FA SLNs was in the range of 212 to 620 nm, zeta potential of-20 mV, drug entrapment efficiency of 72%. *In vitro* drug release for the prepared formulation showed 53% over 48 h.

Conclusion: The optimized DZN-FA SLNs could aid in a better formulation targeting colon cancer cells, thereby reducing systemic effects. The optimized DZN-FA SLNs have demonstrated excellent inhibitory properties on Caco-2 cells, with an IC_{50} value of 10 µg/ml, offering a promising innovation in cancer treatment by providing targeted and effective therapy for colon cancer while minimizing the impact on normal cells.

Keywords: Colon cancer, Daidzein, Folic acid, Solid lipid nanoparticles, Microemulsion, Caco-2 cells

DOI: https://dx.doi.org/10.22159/ijap.2024v16i2.49879 Journal homepage: https://innovareacademics.in/journals/index.php/ijap

INTRODUCTION

Colon cancer is a lethal malignancy with confined treatment strategies. In 2020, colon cancer accounted for 1.93 million new cases and 9,40,000 deaths worldwide, making it the third most common cancer and second leading cause of cancer-related mortality globally [1]. Although chemotherapy is widely used in the treatment, various reports show that it causes systemic toxicity, lack of specificity and bioavailability, which limits its treatment, attacking both healthy cells and cancer cells and causing systemic toxicity to the patients [2]. Conventional cancer therapy typically involves non-specific anti-neoplastic agents that affect both cancerous and healthy cells. To enhance drug delivery to cancer cells while minimizing toxicity to adjacent normal cells, improved targeting moieties and the development of drug resistance over time are required. This approach aims to reduce systemic toxicity and mitigate undesirable side effects. Hence, there is a pressing need for novel strategic approaches to enhance drug delivery and target cancer cells more effectively [3].

Daidzein, a natural flavonoid, has received significant attention due to its potential anticarcinogenic and antiproliferative effects and possible role in many signal transduction pathways [4, 5]. A possible mechanism involves inhibitory effects on tyrosine kinases and DNA topoisomerases, induction of apoptosis, and modulation of signal transduction pathways like PI_3K/Akt and Wnt/β-catenin [6]. Daidzein, a poorly water-soluble drug, presents a challenge in drug transport to the systemic circulation and the site of action, resulting in limited pharmacological effects and poor bioavailability [7]. This is a significant concern for formulation scientists. Solid lipid nanoparticles (SLNs) will be developed to overcome these issues as they are biodegradable, offer low toxicity, low dosage requirement, overcome first-pass metabolism, enhance orally administered drug reaching into the systemic circulation, and exhibit sustained drug release at periodic intervals [8]. Active targeting of anticancer agents leverages specific interactions between receptors present abundantly on the surface of tumor cells and ligands attached to the polymer backbone [9]. This approach capitalises on the enhanced permeability and retention (EPR) effect and significantly improves the therapeutic index by facilitating receptor-mediated tumor-cell uptake [10, 11]. Many studies have indicated folate receptor overexpression in colon cancer cells, but its expression is limited to the apical surface of epithelial cells in normal tissues [12]. Hence, folate-conjugated nanoparticles will be prepared so that on reaching their targeting site, they bind to its receptors and enhance drug accumulation at cancerous tissues thereby, receptor-mediated endocytosis occurs [13, 14].

This study aims to optimize prepared SLNs using statistically experimental design methodology using Box-Behnken design using a three-factor two-level design employing independent variables such as solid lipid ratio, surfactant concentration and homogenization speed on dependent variables: particle size and entrapment efficiency to study the effect of formulation components on responses and exploring quadratic response surface plots and study their physicochemical characterisation properties [15, 16].

MATERIALS AND METHODS

Materials

Daidzein was purchased from Sigma Aldrich (Mumbai, India), stearic acid, pluronic F-127, and Tween 80 from Himedia Labs (India). EDC and NHS were procured from Merck Co. (Darmstadt, Germany), and folic acid was procured from Sigma–Aldrich (St Louis, MO, USA). All the reagents and chemicals used in the study were of analytical grade.

Preparation of daidzein solid lipid nanoparticles (SLNs)

A microemulsion technique was employed for the preparation of daidzein solid lipid nanoparticles. Briefly, the organic phase containing solid lipid stearic acid (250 mg) was heated at 65 °C in a water bath. Daidzein drug dissolved in ethanol (10 ml) was added to the organic phase. The heated aqueous phase containing pluronic F-127 dissolved in 30 ml distilled water was added to the organic

phase dropwise, forming W/O emulsion, after which this hot microemulsion was dispersed in an ice bath and subjected to high shear homogenizer at 10,000 RPM. Later, the solution was subjected to probe sonication for 30 min with 28% amplitude, centrifuged and the resultant supernatant was mixed with 5% mannitol, freeze-dried and lyophilized [17].

Conjugation of folic acid to solid lipid nanoparticles

A regular procedure involved dissolving 20 mg of folic acid (FA) in 8 ml of 1 PBS buffer at pH 7.4, forming a clear yellow solution. 4 ml of an aqueous solution containing 0.0260 g (0.1356 mmol) of EDC and 0.0156 g (0.1355 mmol) of NHS was added to activate the FA solution. This activated FA solution was subsequently conjugated to the surface of stearic acid-containing solid lipid nanoparticles. The mixture underwent 24 h of sonication at room temperature. The solution was then dialysed using a membrane with a molecular weight cutoff (MWCO) of 1000 Da in deionised (DI) water for 24 h to eliminate excess FA. The resulting product was subsequently subjected to lyophilization, yielding a yellow powder product with an approximate yield of 40% [18].

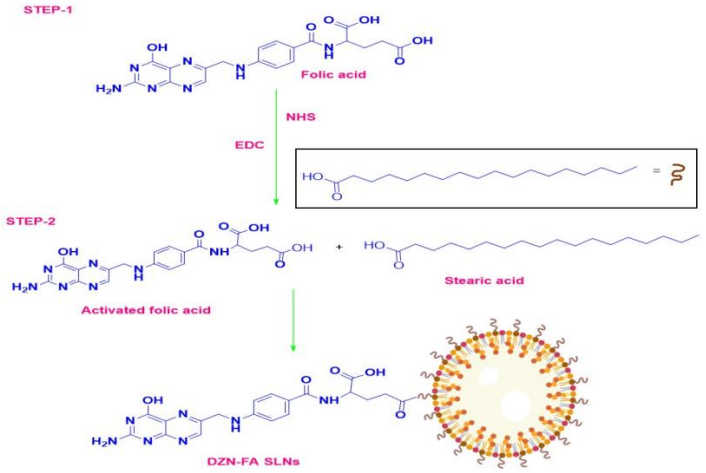

Fig. 1: Schematic illustration of daidzein conjugated folic acid solid lipid nanoparticles

Statistical experimental design

The formulation optimization used Design-Expert software (Design Expert 13, Stat Ease Inc., Minneapolis, USA). Solid lipid (X1), surfactant (X2), and homogenization speed (X3) were chosen as independent variables, with low, medium, and high values assigned based on their significant influence on critical material attributes (CMAs), impacting particle size (Y1) and entrapment efficiency (Y2). The coded values of independent variables were tabulated in table 1. This design explores independent variables main effects and potential interactions on formulation characteristics, aiming to maximise entrapment efficiency and minimise particle size. Box-Behnken was selected because it was efficient and required fewer runs than the central composite design. ANOVA was used for statistical validation and to generate polynomial equations provided by design expert software [19–21].

The response generated after inputting variables was fit into various models like linear, quadratic, cubic and 2FI. Significance was determined with a *P*-value below 0.05. Design Expert software generated 3D response plots through a comprehensive grid search across the experimental region. Experimental values were quantitatively compared to the predicted values obtained from these response plots. Data was analyzed using Design Expert software version 13.0 to get polynomial equations, and model evaluation involved assessing statistical coefficients and R^2 values. 3D surface plots were employed to visualize the relationships between variables and responses.

Table 1: Variables and their levels for preparation of daidzein conjugated folic acid solid lipid nanoparticles

Variables				**Level of variables**	
Independent variables (Uncoded)	**Coded**	**Coded level**	**Low**	**Medium**	**High**
Solid lipid (mg)	A	-1	250	500	750
Surfactant (%)	B	0	1	1.5	2
Homogenization speed (RPM)	C	1	5000	7000	10000
Dependent factors			**Constraints**		
Particle size(nm) (Y_1)			Minimum		
Entrapment efficiency (%) (Y_2)			Maximum		

Analysis of particle size, zeta potential and polydispersity index

All samples were diluted in a 1:10 ratio with millipore water and filtered through a 0.45 µm membrane filter to get optimal counts. Particle size, zeta potential and PDI were measured using an Anton Paar Litesizer 500(Malvern instrument, UK) at a scattering angle of 90 °C. The diluted dispersion was placed in a polystyrene cuvette with a path length of 10 mm and allowed to equilibrate for 120 seconds [22].

Drug entrapment efficiency

The percentage entrapment efficiency (%EE) of the optimized Daidzein conjugated folic acid nanoparticles (DZN-FA SLNs) was determined using the ultracentrifugation method. A 10 ml SLN dispersion was centrifuged at 15,000 rpm for 30 min at room temperature using equipment from Remi Instruments Pvt. Ltd, India. % EE was calculated as the difference between the total drug used in SLN preparation and the drug found in the supernatant, measured at λ_{max} 248 nm using a Shimadzu 1800 UV-spectrophotometer [23].

$$\% \text{ Entrapment efficiency} = \frac{\text{DZN (total drug)} - \text{DZN (free drug)}}{\text{DZN (total drug)}} \text{ x } 100$$

FTIR spectroscopy analysis

Infrared spectra of pure drug and combination with excipients (solid lipid, surfactant) and conjugation (EDC and folic acid) were assessed to find out possible interactions in optimized formulation with the

Perkin Elmer instrument (Perkin Elmer, USA). Powder samples were scanned over a range of 700-4000 cm^{-1}.

SEM analysis of prepared SLNs

The prepared solid lipid nanoparticle samples were examined for the morphological studies (size and shape) using a high-resolution scanning electron microscope (ZEISS SIGMA VP Scanning Electron Microscope) at 30 kV. To prepare the samples for observation, they were affixed to mounts using double-sided adhesive tapes and coated with a layer of gold-palladium alloy (150–200 A °). The SEM was operated at a 30 kV acceleration voltage, with a working distance between 12-14 mm. The samples were observed at a magnification between 350x and 1500x [24].

***In vitro* drug release**

DZN-FA SLN drug release was done using a dialysis bag (MWCO 12-14kDa) method in pH 7.4 PBS. The dialysis bag retained SLNs, allowing free drugs to dissolve in the media. Before the experiment started, the dialysis bag was soaked in double distilled water for 24 h. Ten millilitres of DZN-FA SLNs were placed in the bag and then sealed at one end. The bag was immersed in the beaker with 50 ml of fluid on a magnetic stirrer at 37 °C (100 rpm). Drug samples (1 ml) were withdrawn at various time points (0.5, 1, 2, 3, 4, 8, 24, 48 h), and fresh dialysis medium was added to uphold sink conditions, and then the filtrate was analyzed using a UV spectrophotometer at a wavelength of 248 nm [25].

***In vitro* cell viability assay-MTT assay**

Caco-2 cells were cultured in RPMI-1640 with 10% FBS, 1% penicillin-streptomycin, and 2g/l sodium bicarbonate at 37 °C in a humidified atmosphere. The cytotoxicity of DZN-FA SLNs was evaluated using MTT assay. Briefly, cells were seeded at a density of $5x10^3$cells/well in a 96-well plate and were treated with different concentrations (0, 10, 20, 30, 40, 50µg/ml) of DZN, DZN-SLNs and DZN-FA SLNs (dissolved in 0.5% DMSO) and blank. After treatment, medium was removed and 50 µl of 5 mg/ml MTT in PBS was added. Following 4h incubation at 37 °C, formazan crystals were dissolved in DMSO, and absorbance was measured at 570 nm using a spectrophotometric microplate reader (ELx 800, Biotek, CA).

Stability studies

To assess the stability and physicochemical properties of the formulation, the optimized DZN-FA SLNs underwent a stability study in triplicate. They were stored at three conditions: 4±2 °C, 25±2 °C/60±5% relative humidity (RH) and 40±2 °C/75±5% RH in a stability chamber (Remi Instruments Ltd). Parameters like particle size, zeta potential, PDI, % EE and % drug release were quantified at 1, 3 and 6 mo intervals.

RESULTS AND DISCUSSION

Enormous research has been carried out to develop SLNs using various techniques. In this study, we employed the process of microemulsion followed by high shear homogenization and probe sonication for preparing SLNs in a simple, reliable and economical way. The microemulsions are formed when heated to a temperature higher than the melting point of lipid, thus allowing to combine with a liquid that is solid at room temperature.

Optimization of SLNs by box-behnken design

13 runs were generated using Box-Behnken design in Design Expert software. These runs involved different independent variables and responses at various levels (low, medium, high), focusing on optimizing solid lipid nanoparticles key variables with a goal of small particle size and high entrapment efficiency. Linear and 2FI models were found to best-fit models for the dependent variables. The results of the 13 experimental runs for the DZN-FA SLNs, regression analysis summary for responses, and ANOVA for the response models (R1, R2) are enlisted in tables 2-5.

Table 2: Observed responses of 13 run experimental designs according to box-behnken design

	Factor 1	Factor 2	Factor 3	Response 1(Y1)	Response 2 (Y2)
Run	A: solid lipid(%w/w)	B: Surfactant concentration (%)	C: Homogenization speed(rpm)	Particle size(nm)	Entrapment efficiency (%)
1	0.5	1.25	9000	212±0.88	57.92±1.45
2	2	1.25	3000	596±1.32	53.45±1.43
3	0.5	0.5	6000	455±0.44	48.82±0.88
4	0.5	2	6000	308±1.64	61.27±0.21
5	2	2	6000	444±0.81	68.42±1.56
6	1.25	0.5	9000	408±1.45	51.99±0.53
7	0.5	1.25	3000	480±1.53	48.92±1.42
8	2	1.25	9000	388±0.86	65.91±1.85
9	1.25	2	9000	256±0.32	71.66±0.32
10	1.25	0.5	3000	620±2.11	45.88±0.78
11	1.25	2	3000	486±1.32	56.44±0.11
12	2	0.5	6000	579±1.55	51.66±1.43
13	1.25	1.25	6000	433±0.63	55.43±1.77

Values are in mean±SD, n=3

Effect on particle size

The formulation was run for 13 runs. Particle size ranged from 212 to 620 nm for various factor levels. The independent factors affecting particle size were solid lipid ratio (% w/w), surfactant concentration (%) and homogenization speed (rpm) (p<0.001, table 3 and fig. 2). In a polynomial equation, a positive sign indicates a synergistic relationship, where the variables interact positively to have a greater combined effect. On the other hand, a negative sign indicates an antagonistic relationship, where variables interact negatively, resulting in a combined effect that is less than the sum of individual effects. The best-fitting model was found to be a linear model. The effect of particle size can be equated using the following quadratic equation:

Particle size (Y1) =+435.77+69A+71B-114.75C+3A+15AC-4.50BC . Eq.1

The model F value of 90.19, with a significance level (P<0.0001), confirmed its significance. In this case, model terms A and B were significant model terms. Positive coefficients of B and C indicated a synergistic effect on particle size, while negative coefficients of C and BC indicated an antagonistic effect on particle size. The predicted R^2 of 0.9638 aligns reasonably well with adjusted R^2 of 0.9781, indicating model suitability for prediction of particle size. The 3-dimensional response surface plots showed the impact of different formulation variables on particle size (Y1). The average particle size ranged between 212 to 620 nm, which determined comprehensive effects as an increase in solid lipid ratio and surfactant ratio increased particle size, while the increase in surfactant concentration and homogenization speed caused a reduction in particle size. The effect of particle size on various factors has been illustrated in fig. 2.

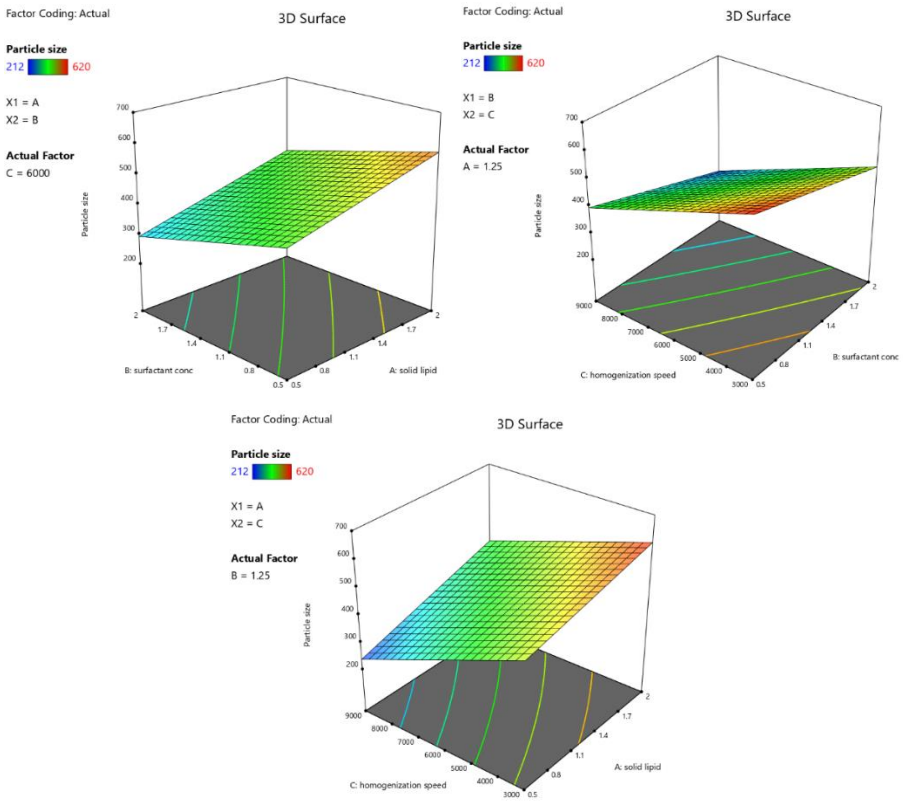

Fig. 2: 3D response plots showing the effect of independent variables on particle size

Effect on entrapment efficiency

According to results obtained from experiments performed on 13 runs, entrapment efficiency varied from 45-71%. It was mainly influenced based on independent variables (P<0.0001). The polynomial equation (Eq 2) shows that all the independent variables have positive impacts on entrapment efficiency, which can be depicted below.

$$EE(Y2) = +56.75+2.81A+7.43B+5.35C+1.08AB+0.8650AC+2.28BC. \quad Eq.2$$

The model F value of 135.82 revealed that the model was statistically significant (*P*<0.0001). Model terms A, B, C, AB, AC, and BC were significant in this case. The positive effect was shown on all the coefficient variables, indicating a synergistic effect. The best-fitting model for entrapment efficiency was the 2FI model. The predicted R^2 of 0.9692 is in reasonable agreement with the adjusted R^2 of 0.9854, confirming the models suitability for predicting entrapment efficiency. Additionally, 3D response surface plots visually illustrate how various formulation variables impact entrapment efficiency (Y2). The entrapment efficiency ranged between 45-71%, which determined positive impact effects as an increase in solid lipid ratio and surfactant ratio increased entrapment efficiency. At the same time, an increase in surfactant concentration and homogenization speed also caused an increase in entrapment efficiency. The effect of entrapment efficiency on various factors has been illustrated in fig. 3.

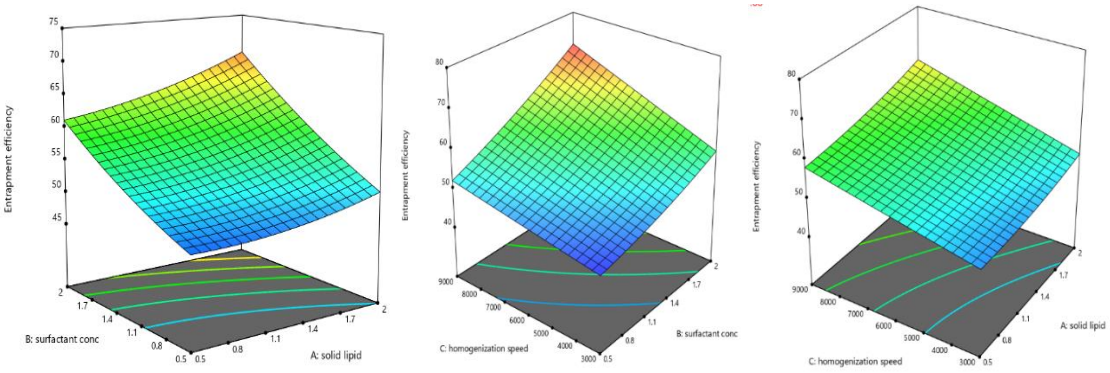

Fig. 3: 3D response plots showing the effect of independent variables on entrapment efficiency

Variable interaction and point prediction

The degree of variation from independent variables and their responses were evaluated by perturbation plots, which indicate that an increase in solid lipid and surfactant causes an increase in particle size. In contrast, the increase in homogenization speed and solid lipid ratio causes a decrease in particle size (fig. 2). Similarly, an increase in solid lipid ratio caused an increase in entrapment efficiency. An increase in homogenization speed and surfactant ratio caused an increase in entrapment efficiency (fig. 3). The software

point prediction was employed to optimize both particle size and entrapment efficiency. The formulations best-fit the criteria were selected and optimized to achieve minimal particle size and maximum entrapment efficiency. The low % prediction error values validated the obtained polynomial equations and demonstrated the applicability of response surface methodology (RSM). Therefore, optimizing software has given values for solid lipid as 1%(w/w), surfactant concentration as 1(%), and 5500 rpm. Estimated particle size and entrapment efficiency for optimal SLN preparation were 260 nm and 75%, respectively.

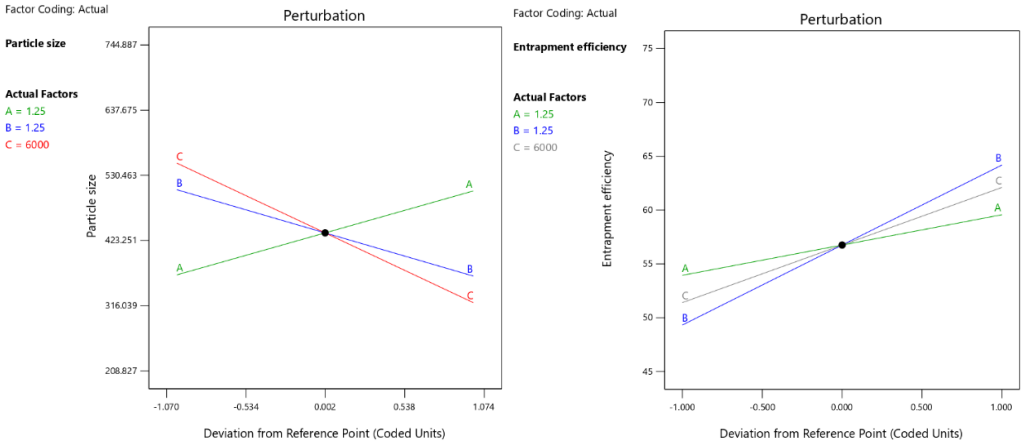

4(a) **4(b)**

Fig. 4: (a) perturbation plots on particle size, (b) Perturbation plots on entrapment efficiency

Table 3: Analysis of variance for the response particle size (R1)

Source	Sum of squares	df	Mean square	F-value	p-value	
Model	1.85E+05	6	30795.58	90.19	<0.0001	significant
A-solid lipid	38088	1	38088	111.54	<0.0001	
B-surfactant conc	40328	1	40328	118.1	<0.0001	
C-homogenization speed	1.05E+05	1	1.05E+05	308.49	<0.0001	
AB	36	1	36	0.1054	0.7564	
AC	900	1	900	2.64	0.1556	
BC	81	1	81	0.2372	0.6435	
Residual	2048.81	6	341.47			
Cor total	1.868E+05	12				

Table 4: Analysis of variance for the response entrapment efficiency (R2)

Source	Sum of squares	df	Mean square	F-value	p-value	
Model	762.23	6	127.04	135.82	<0.0001	significant
A-solid lipid	63.34	1	63.34	67.72	0.0002	
B-surfactant conc.	441.64	1	441.64	472.17	<0.0001	
C-homogenization speed	228.87	1	228.87	244.69	<0.0001	
AB	4.64	1	4.64	4.97	0.0674	
AC	2.99	1	2.99	3.2	0.1239	
BC	20.75	1	20.75	22.18	0.0033	
Residual	5.61	6	0.9353			
Cor Total	767.85	12				

Table 5: Summary of the results of regression analysis of responses

Model	R^2	Adjusted R^2	Predicted R^2	Adequate precision	SD	% CV	Remark
Response (Y1)							
2FI	0.0001	0.9781	0.9389	28.0241	18.48	4.24	
Linear	0.9836	0.9781	0.9638	36.2869	18.46	4.24	Suggested
Quadratic	0.9985	0.9941	0.8533	48.0955	9.57	2.2	
Response (Y2)							
2FI	0.9927	0.9854	0.9692	36.0126	0.9671	1.7	Suggested
Linear	0.9557	0.941	0.9046	23.7061	1.94	3.42	
Quadratic	0.9988	0.9951	0.8322	52.2731	0.5575	0.9823	

Physicochemical characterization of DZN-FA SLNs

The optimized formulations particle size, polydispersity index (PDI), and zeta potential are illustrated in fig. 4. The average particle size, PDI and zeta potential were 223 nm, 20.3% and-20 mV. These results prompted that narrow particle size indicates consistent nature, uniformity and stability of the formulation and zeta potential revealed good electrostatic interaction between nanoparticles [26].

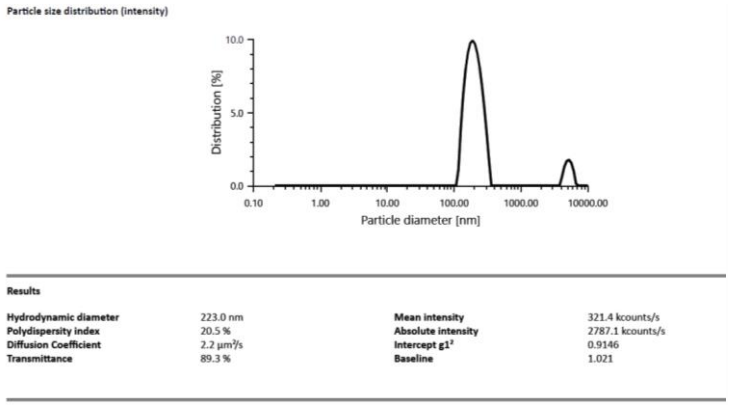

Fig. 5: Particle size and PDI of optimized DZN-FA SLNs

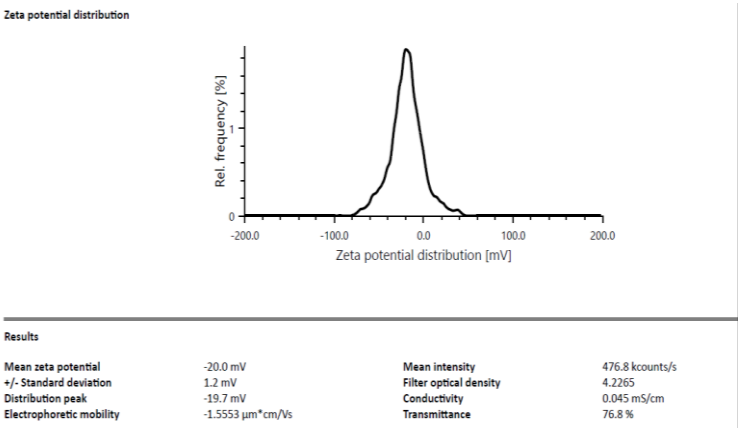

Fig. 6: Zeta potential of optimized DZN-FA SLNs

Determination of drug entrapment efficiency

The entrapment efficiency of optimized DZN-FA SLNs and DZN SLNs was 72±2 % and 69±3% respectively [27].

FTIR spectroscopy measurements

The spectral pattern of the prepared DZN-FA SLNs was confirmed through FTIR analysis. The recorded spectra are shown in fig. 3. The spectrum of daidzein reveals several absorption peaks attributed to its primary functional groups. Broad Peaks observed at 3158 cm^{-1} attributed to presence of the amide (NH_2) group and peaks at 1629 cm^{-1}, 1387 cm^{-1},1278 cm^{-1}, and 1237 cm^{-1}shows the presence of amide stretch, O-H stretch, C-O stretch. Similarly, stearic acid shows peaks at 2955 cm^{-1}, 2915 cm^{-1}, 2848 cm^{-1}, 1697 cm^{-1}, and 1430 cm^{-1}attributed to presence of C-H stretch, primary amide stretch, secondary amide stretch, C=O stretch and O-H stretch. EDC exhibits characteristic peaks at 2916 cm^{-1}, 1695 cm^{-1}, and 1471 cm^{-1}, depicting the presence of O-H stretch, C=O stretch, and C-H stretch. The peaks for folic acid were observed at 2915 cm^{-1} and 1694 cm^{-1}, confirming the presence of O-H stretch C=O stretch. DZN SLNs showed peaks at 2955 cm^{-1}, 2915 cm^{-1}, 2347 cm^{-1}, 1694 cm^{-1}confirming the presence of N-H stretch, O-H stretch, carboxyl group and C=O (aldehyde) group (fig. 7(ii)). The prepared DZN-FA SLNs formulation showed the peaks at 3506 cm^{-1}, 2914 cm^{-1}, 1711 cm^{-1}, 1470.97 cm^{-1}, 1248.07 cm^{-1}attributed to the presence of NH_2 stretch, primary amide, O-H stretch, C-H stretch, C-N stretch (fig. 7(i)). These findings suggest that DZN-FA SLNs are molecularly dispersed with the lipids in SLNs [28].

SEM of prepared DZN SLNs and DZN-FA SLNs

SEM analysis of the daidzein SLNs and folic acid-conjugated daidzein SLNs revealed their shape and surface morphology. The SEM results indicated a spherical shape and a smooth surface for the formulation. The nanoparticles exhibited a spherical shape for DZN SLNs and DZN-FA SLNs, with a size ranging approximately between 200-300 nm. This observation correlates with the particle size obtained from the Anton Paar Litesizer instrument.

***In vitro* drug release**

Fig. 5 illustrates *in vitro* drug release profiles of daidzein release from DZN-FA SLNs, DZN SLNs and DZN suspension. DZN initially displayed a burst release of 50%, while DZN-FA SLNs and DZN SLNs exhibited sustained release patterns, reaching 30% at 12 h and 80% at 72 h. This sustained release pattern was due to stearic acid diffusing property through the lipoidal membrane. The initial burst release of up to 30% from SLNs was attributed to the drug being entrapped in the outer stratum or adsorbed on the surface. *In vitro* drug release of various formulations was conducted using different kinetic models, including zero order, first order, Higuchi, Korsmeyer–Peppas and Hixson–Crowell. Both formulations best fit the Higuchi model, indicated by the highest linearity (R^2 = 0.987) confirmed by comparing obtained regression coefficient values for various kinetic models. The release follows non-Fickian diffusion, involving diffusion and dissolution of the DZN-FA SLNs matrix [29].

***In vitro* cell viability assay-MTT assay**

MTT assay assessed anti-proliferative effects on DZN, DZN SLNs and DZN-FA SLNs in colon cancer (Caco-2) cell lines. The data analysis of the cytotoxicity assay revealed that the DZN-FA SLNs IC_{50} value was around 10 µg/ml, whereas DZN SLNs and DZN were 30 and 40 µg/ml. The results showed that DZN-FA SLNs exhibited better cytotoxic activity when compared with DZN SLNs and DZN. Thus, the conjugation to folic acid has effectively delivered the drug onto cancer cells through folate receptor-mediated endocytosis.

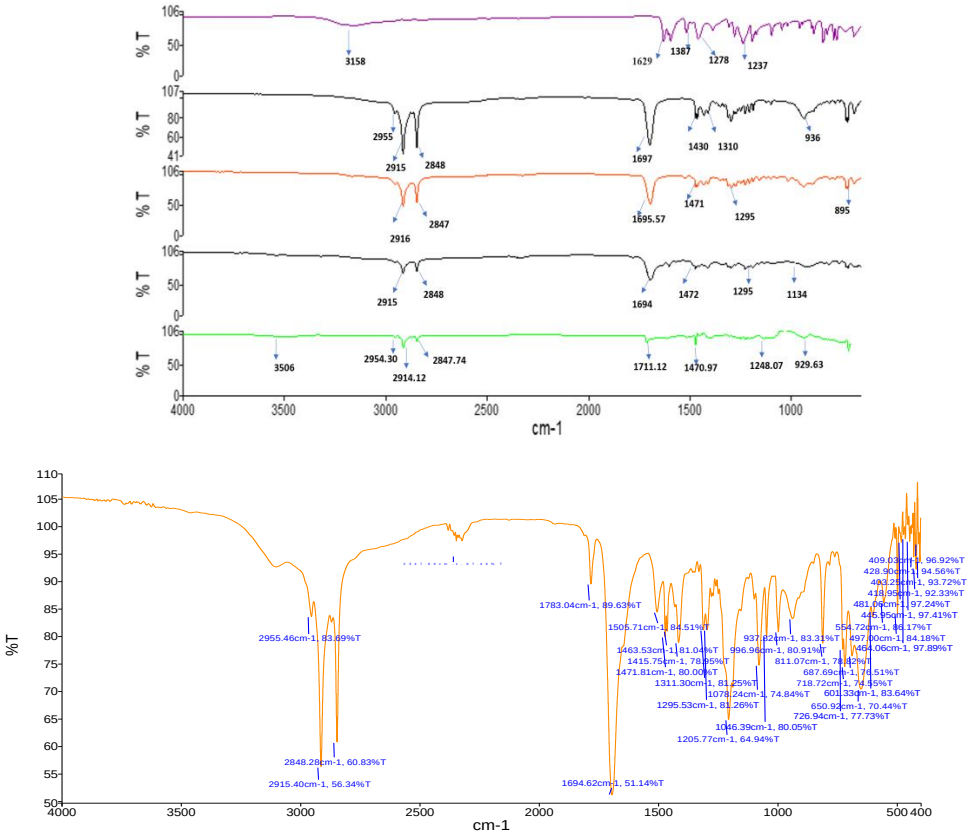

Fig. 7: (i) FTIR study of DZN-FA SLNs (A) Daidzein (B) Stearic acid (C) EDC (D) Folic acid (E) DZN-FA SLNs (ii) DZN SLNs

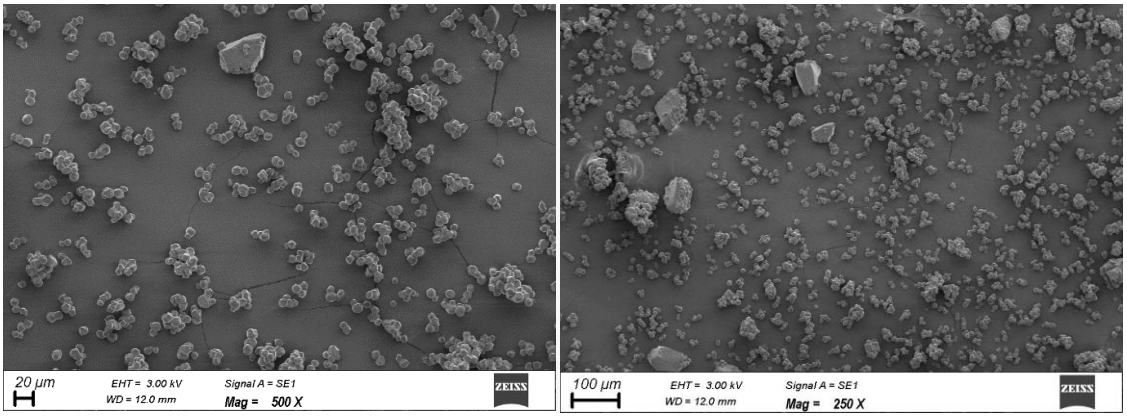

A **b**

Fig. 8: SEM image of (a) DZN-SLNs and (b) DZN-FA SLNs

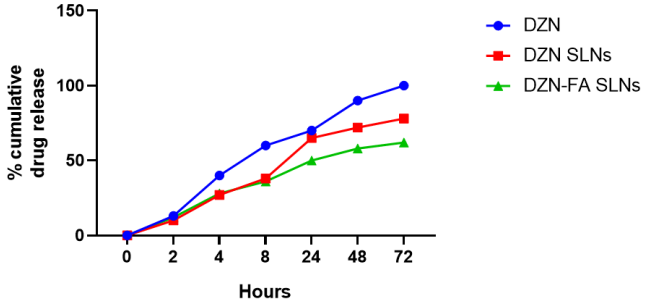

Fig. 9: *In vitro* drug release of DZN from free DZN, DZN SLNs and DZN-FA SLNs by dialysis bag method at pH 7.4. Data shown are mean±SD (n=3). Error bars were omitted for clear presentation

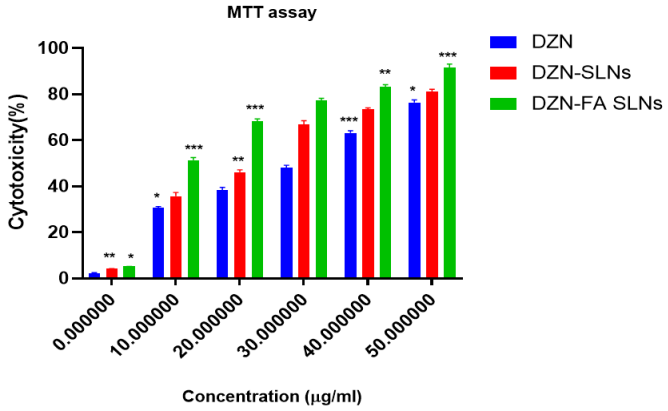

Fig. 10: MTT assay of DZN, DZN SLNs and DZN-FA SLNs after treatment with Caco-2 cells. Data was analyzed by applying two-way ANOVA with Tukey's posthoc tests; **P* value<0.05, ***P* value<0.01, and ****P* value<0.001. Asterisks (*) indicate statistically significant difference compared with their respective control, where *P*<0.05 is considered as significant

Accelerated stability studies

The results depict that prepared SLNs were stable, and there was a slight increase in particle size, zeta potential and entrapment efficiency during the 30-day time period at 4±2 °C and 25±3 °C. The particle size increased from 220±2 nm to 225±3 nm, zeta potential increased from-20±0.2 mV to-22±0.5 mV, and entrapment efficiency of 73±4% was observed. This indicates good physical stability against aggregation and higher zeta potential indicates strong electrostatic interaction between positive and negative electrons exhibiting good aggregation patterns [30].

Table 6: Stability studies

Storage conditions: 40 °C±2 °C/75%RH±5%RH					
Sample	**sample time point (days)**	**Appearance**	**Particle size**	**Zeta potential**	**Entrapment efficiency**
DZN-FA SLNs	0 d	white colour	220±2 nm	-20±0.2 mV	72%
	30 d	white colour	225±2 nm	-22±0.5 mV	73.20%

Data is given in mean±SD, n=3

CONCLUSION

In the current research, novel formulation containing daidzein-conjugated folic acid solid lipid nanoparticles was developed and optimized using design expert software. DZN-FA SLNs were prepared using the microemulsion method, conjugated with folic acid and optimized for small particle size and high entrapment efficiency. Spherical images were observed in SEM, and the drug was molecularly dispersed in FTIR studies. *In vitro* drug release exhibited sustained release patterns by prolonging drug pharmacological activity, improving pharmacokinetics. *In vitro* cytotoxicity assay demonstrated that DZN-FA SLNs have shown dose-dependent cytotoxicity at 10 µg/ml through receptor-mediated endocytosis. This novel approach is a better option for formulating and targeting colon cancer.

ACKNOWLEDGEMENT

The authors would like to thank the Department of Science and Technology-Fund for Improvement of Science and Technology Infrastructure (DST-FIST), Promotion of University Research and Scientific Excellence (DST-PURSE) and Department of Biotechnology-Boost to University Interdisciplinary Life Science Departments for Education and Research programme (DBT-BUILDER) for the facilities provided for conducting the research.

FUNDING

No funding was received for this work.

AUTHORS CONTRIBUTIONS

Syed Suhaib Ahmed-Conceptualization, validation, Writing–Original Draft Preparation and Data curation. Mohd Abdul Baqi-Data curation, methodology, Writing–Review and Editing. Mohd Zubair Baba-Data curation, Writing–Review and Editing. Natarajan Jawahar–Conceptualization, Formal Analysis, validation and supervision.

CONFLICT OF INTERESTS

There is no conflict of interest.

REFERENCES

1. Xi Y, Xu P. Global colorectal cancer burden in 2020 and projections to 2040. Transl Oncol. 2021 Oct 1;14(10):101174. doi: 10.1016/j.tranon.2021.101174, PMID 34243011.
2. Conde J, Oliva N, Zhang Y, Artzi N. Local triple-combination therapy results in tumour regression and prevents recurrence in a colon cancer model. Nat Mater. 2016 Oct;15(10):1128-38. doi: 10.1038/nmat4707, PMID 27454043.
3. Hou Y, Jin J, Duan H, Liu C, Chen L, Huang W. Targeted therapeutic effects of oral inulin-modified double-layered nanoparticles containing chemotherapeutics on orthotopic colon cancer. Biomaterials. 2022 Apr 1;283:121440. doi: 10.1016/j.biomaterials.2022.121440, PMID 35245731.
4. Tuli HS, Tuorkey MJ, Thakral F, Sak K, Kumar M, Sharma AK. Molecular mechanisms of action of genistein in cancer: recent advances. Front Pharmacol. 2019;10:1336. doi: 10.3389/fphar.2019.01336, PMID 31866857.
5. Kim SH, Kim CW, Jeon SY, Go RE, Hwang KA, Choi KC. Chemopreventive and chemotherapeutic effects of genistein, a soy isoflavone, upon cancer development and progression in preclinical animal models. Lab Anim Res. 2014 Dec;30(4):143-50. doi: 10.5625/lar.2014.30.4.143, PMID 25628724.
6. Li H, Zhang M, Wang Y, Gong K, Yan T, Wang D. Daidzein alleviates doxorubicin-induced heart failure via the SIRT3/FOXO3a signaling pathway. Food Funct. 2022 Sep 22;13(18):9576-88. doi: 10.1039/d2fo00772j, PMID 36000402.

7. Senft D, Ronai ZEA. Adaptive stress responses during tumor metastasis and dormancy. Trends Cancer. 2016 Aug;2(8):429-42. doi: 10.1016/j.trecan.2016.06.004, PMID 27868104.
8. Chan KKL, Siu MKY, Jiang YX, Wang JJ, Leung THY, Ngan HYS. Estrogen receptor modulators genistein, daidzein and ERB-041 inhibit cell migration, invasion, proliferation and sphere formation via modulation of FAK and PI3K/AKT signaling in ovarian cancer. Cancer Cell Int. 2018 May 1;18(1):65. doi: 10.1186/s12935-018-0559-2, PMID 29743815.
9. Jaiswal PK, Keserwani S, Chakrabarty T. Lipid-polymer hybrid nanocarriers as a novel drug delivery platform. Int J Pharm Pharm Sci. 2022 Apr 1:1-12. doi: 10.22159/ijpps.2022v14i4.44038.
10. Rajpoot K, Jain SK. Colorectal cancer-targeted delivery of oxaliplatin *via* folic acid-grafted solid lipid nanoparticles: preparation, optimization, and *in vitro* evaluation. Artif Cells Nanomed Biotechnol. 2018 Aug 18;46(6):1236-47. doi: 10.1080/21691401.2017.1366338, PMID 28849671.
11. Ravanfar R, Tamaddon AM, Niakousari M, Moein MR. Preservation of anthocyanins in solid lipid nanoparticles: optimization of a microemulsion dilution method using the placket–burman and box–behnken designs. Food Chem. 2016;199:573-80. doi: 10.1016/j.foodchem.2015.12.061, PMID 26776010.
12. Bhosale RR, Janugade BU, Chavan DD, Thorat VM. Current perspectives on applications of nanoparticles for cancer management. Int J Pharm Pharm Sci. 2023 Nov 1:1-10. doi: 10.22159/ijpps.2023v15i11.49319.
13. Choi IK, Strauss R, Richter M, Yun CO, Lieber A. Strategies to increase drug penetration in solid tumors. Front Oncol. 2013;3:193. doi: 10.3389/fonc.2013.00193, PMID 23898462.
14. Yoo J, Park C, Yi G, Lee D, Koo H. Active targeting strategies using biological ligands for nanoparticle drug delivery systems. Cancers. 2019 May;11(5):640. doi: 10.3390/cancers11050640, PMID 31072061.
15. Yasir M, Sara UVS. Preparation and optimization of haloperidol-loaded solid lipid nanoparticles by box–behnken design. J Pharm Res. 2013;7(6):551-8. doi: 10.1016/j.jopr.2013.05.022.
16. Gidwani B, Vyas A. Preparation, characterization, and optimization of altretamine-loaded solid lipid nanoparticles using box-behnken design and response surface methodology. Artif Cells Nanomed Biotechnol. 2016;44(2):571-80. doi: 10.3109/21691401.2014.971462, PMID 25363752.
17. Kotmakçı M, Akbaba H, Erel G, Ertan G, Kantarcı G. Improved method for solid lipid nanoparticle preparation based on hot microemulsions: preparation, characterization, cytotoxicity, and hemocompatibility evaluation. AAPS PharmSciTech. 2017 May;18(4):1355-65. doi: 10.1208/s12249-016-0606-z, PMID 27502405.
18. Yassemi A, Kashanian S, Zhaleh H. Folic acid receptor-targeted solid lipid nanoparticles to enhance the cytotoxicity of letrozole through induction of caspase-3 dependent-apoptosis for breast cancer treatment. Pharm Dev Technol. 2020 Apr 20;25(4):397-407. doi: 10.1080/10837450.2019.1703739, PMID 31893979.
19. Ngwuluka NC, Kotak DJ, Devarajan PV. Design and characterization of metformin-loaded solid lipid nanoparticles for colon cancer. AAPS PharmSciTech. 2017 Feb;18(2):358-68. doi: 10.1208/s12249-016-0505-3, PMID 26975870.
20. Devi AR, MV. Donepezil hydrochloride loaded solid lipid nanoparticles: formulation, *in vitro–in vivo* pharmacokinetic and pharmacodynamics evaluation. Int J App Pharm. 2022 May 7:125-34. doi: 10.22159/ijap.2022v14i3.44145.
21. Surve C, SINGH R, Banerjee A, Patnaik S, Shidhaye S. Formulation and QBD based optimization of methotrexate-loaded solid lipid nanoparticles for an effective anti-cancer treatment. Int J App Pharm. 2021 Sep 7:132-43. doi: 10.22159/ijap.2021v13i5.42373.
22. Padmasree M, Vishwanath BA. Development and characterization of pegylated capecitabine liposomal formulations with anticancer activity towards colon cancer. Int J App Pharm. 2022;14(2):135-42. doi: 10.22159/ijap.2022v14i2.43658.
23. Lee PC, Lin CY, Peng CL, Shieh MJ. Development of a controlled-release drug delivery system by encapsulating oxaliplatin into SPIO/MWNT nanoparticles for effective colon cancer therapy and magnetic resonance imaging. Biomater Sci. 2016 Nov 15;4(12):1742-53. doi: 10.1039/C6BM00444J, PMID 27722406.
24. Jain A, Jain SK, Ganesh N, Barve J, Beg AM. Design and development of ligand-appended polysaccharidic nanoparticles for the delivery of oxaliplatin in colorectal cancer. Nanomedicine. 2010;6(1):179-90. doi: 10.1016/j.nano.2009.03.002, PMID 19447205.
25. Ozturk K, Mashal AR, Yegin BA, Calıs S. Preparation and *in vitro* evaluation of 5-fluorouracil-loaded PCL nanoparticles for colon cancer treatment. Pharm Dev Technol. 2017 Jul 4;22(5):635-41. doi: 10.3109/10837450.2015.1116565, PMID 26616273.
26. Ibrahim B, Mady OY, Tambuwala MM, Haggag YA. pH-sensitive nanoparticles containing 5-fluorouracil and leucovorin as an improved anti-cancer option for colon cancer. Nanomedicine (Lond). 2022 Mar;17(6):367-81. doi: 10.2217/nnm-2021-0423, PMID 35109714.
27. Prasad S, Dangi JS. Development and characterization of pH-responsive polymeric nanoparticles of SN-38 for colon cancer. Artif Cells Nanomed Biotechnol. 2016 Nov 16;44(8):1824-34. doi: 10.3109/21691401.2015.1105239, PMID 26540095.
28. Tummala S, Satish Kumar MN, Prakash A. Formulation and characterization of 5-fluorouracil enteric coated nanoparticles for sustained and localized release in treating colorectal cancer. Saudi Pharm J. 2015 Jul;23(3):308-14. doi: 10.1016/j.jsps.2014.11.010, PMID 26106279.
29. Yassin AEB, Anwer MdK, Mowafy HA, El-Bagory IM, Bayomi MA, Alsarra IA. Optimization of 5-flurouracil solid-lipid nanoparticles: a preliminary study to treat colon cancer. Int J Med Sci. 2010 Nov 22;7(6):398-408. doi: 10.7150/ijms.7.398, PMID 21103076.
30. Zielinska A, Ferreira NR, Feliczak Guzik A, Nowak I, Souto EB. Loading, release profile and accelerated stability assessment of monoterpenes-loaded solid lipid nanoparticles (SLN). Pharm Dev Technol. 2020 Aug 8;25(7):832-44. doi: 10.1080/10837450.2020.1744008, PMID 32204628.